
Copper K-Shell Emission Cross Sections for Laser–Solid Experiments

Introduction

Fast-electron generation in laser–plasma interactions has long been of interest for a variety of reasons, such as avoiding pre-heat during compression in inertial confinement fusion (ICF), heating the compressed core of an ICF target for fast ignition,¹ generating a shock in an ICF target for shock ignition,² and as a means to produce energetic secondary particles,³ such as protons⁴ and gamma rays.^{5,6}

K-shell emission^{7,8} is a widely used fast-electron diagnostic in laser–solid experiments; it has also been used to provide a source of x rays at a specific energy. The most commonly used emitter in these experiments is copper. K-shell emission is produced when a fast electron knocks out a K-shell electron from an atom in the solid target, which is then replaced by an electron from an outer shell—a transition that leads to the emission of a photon with a characteristic energy in the x-ray band. If the outer shell involved is the L shell, the emission is called K_α ; if it is the M shell, it is called K_β . K_α emission is more probable than K_β emission, so the majority of K-shell diagnostics used in laser–solid experiments rely entirely on K_α emission. It is assumed that the fraction of atoms with missing K-shell electrons, as a result of fast electrons or target heating, is always negligible. A fundamental parameter required when analyzing such measurements is the cross section for K-shell emission by fast electrons. The objective of this article is to identify a simple and accurate published expression for the K-shell emission cross section of copper. The principal motivation for this study was the analysis of K_α -emission diagnostics in laser–solid experiments at peak intensities above 10^{18} W/cm², where the fast-electron energy range of interest is roughly 0.1 to 10 MeV.

This work began with an analysis of time-resolved measurements of total K_α emission in laser–solid experiments;⁷ 20- μ m-thick copper foils were irradiated at normal incidence by \sim 1-ps laser pulses at intensities from 10^{18} to 10^{19} W/cm², and the x-ray emission was recorded using a streaked spectrometer. While looking for a simple expression for the K-shell emission cross section, a confusingly large selection of expressions was found, some of which differed significantly from one another.

A number of nonrelativistic expressions that use $1/E$ in place of $2/m_e v^2$, where E is the kinetic energy, m_e is the electron mass, and v is the velocity, could be immediately discarded as inaccurate at all energies of interest. Closer analysis of the remaining expressions showed that a number of these differences were caused by typing errors, which were identified by comparing the curves given with those in the respective papers, by comparing similar terms used in multiple papers, and by simple physical arguments. The only significant difference that remained was whether the cross section varied as $\ln E$ or $\ln(p^2/2m_e)$, where p is the momentum, which made a difference at relativistic energies. Comparison with the standard expression for electron stopping power suggested a third form, not used in any of the expressions. Furthermore, it suggested a reduction in the cross section at strongly relativistic energies, known as the density-effect correction, which had not been adequately considered. We then turned to measurements of K-shell emission from copper made with electron beams to select the most-accurate expression. Very few measurements in the 0.1- to 10-MeV region were found, so it was not possible to significantly narrow the number of apparently adequate expressions. Too few measurements were found with differences between them that were too large to clearly determine the correct limiting form at relativistic energies. Fortunately, for analyzing our measurements to determine a mean fast-electron energy, where only the relative K_α -emission rate as a function of electron energy was important, these differences were found to be irrelevant. They would be significant if absolute K_α yields were important, for example, to determine the number of fast electrons. To complete our study of K-shell emission, attention was turned to other possible sources of emission in laser–solid experiments, namely keV photons and MeV protons. A brief analysis of K-shell yields for photons and protons showed that the contribution from these sources may not always be entirely negligible, as originally assumed.

Although this work concentrates on copper, which is the most widely used in high-intensity laser–solid experiments and in electron-beam experiments, the basic considerations apply to any material and most of the expressions considered apply

to any material. We have also included some discussion on the variation with atomic number (Z).

In the following sections, the measurements and expressions are presented, followed by a brief discussion of the divergence in the expressions at relativistic energies. Next, the implications of the results for the interpretation of laser–solid experiments are considered, calculating emission rates and yields per electron as a function of electron energy. K-shell yields from other sources in laser–solid experiments that could be confounding factors for fast-electron diagnostics are then considered, namely photons and protons. Finally, our conclusions are presented, followed by the full expressions for the K-shell ionization cross sections in the appendix, with a number of typing errors corrected, and a simple fit for the K-shell emission cross section of copper is proposed.

Electron K-Shell Emission Cross Sections for Copper

K-shell emission cross sections σ_K have been measured using electron beams passing through thin copper films, down to a few nanometers in thickness, to a typical quoted accuracy of better than $\pm 10\%$. The results, however, are always expressed in terms of K-shell ionization cross section σ_{ion} , given by

$$\sigma_K = f_K \sigma_{\text{ion}}, \quad (1)$$

where f_K is fluorescence yield, for which different values have been used; it represents the fact that not all ionization events lead to emission of a photon. To obtain the K-shell emission cross section, it is important to correctly undo this step. Liu *et al.*⁹ give a table of values from papers published before 2000, all modified to a fluorescence yield of 0.441, which simplifies the task. Since then, Llovet *et al.*¹⁰ have published measurements, also using a fluorescence yield of 0.441, and Zhou *et al.*¹¹ have published measurements with an unstated fluorescence yield, but since this publication is from the same group as Liu *et al.*⁹ it seems reasonable to assume that they also used 0.441. We are unaware of any other measurements published before 2013. These values, plotted in Fig. 135.27, are multiplied by the atomic number density of solid copper n_a ($8.49 \times 10^{28} \text{ m}^{-3}$; copper will always refer to solid-density, un-ionized copper), giving what is known as the macroscopic cross section: the mean number of photons emitted per fast electron per meter.

Clearly the differences between various sets of measurements (individual experiments) are far greater than the quoted errors. Llovet *et al.*¹⁰ give a clear explanation of the difference

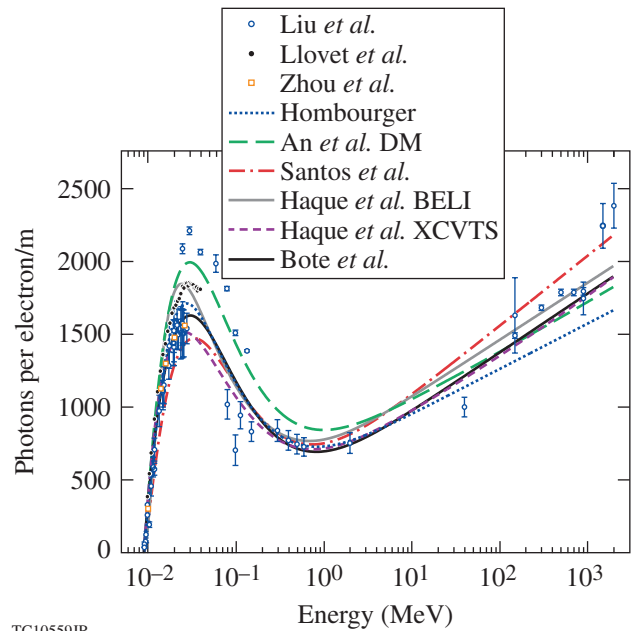


Figure 135.27

Macroscopic K-shell emission cross sections for solid copper. Points are from measurements given by Liu *et al.*,⁹ Llovet *et al.*,¹⁰ and Zhou *et al.*¹¹ Curves are from expressions given by Hombourger,¹⁷ An *et al.*,²² Santos *et al.*,²⁵ Haque *et al.*'s BELI model,¹⁹ Haque *et al.*'s XCVTS model,²⁴ and Bote *et al.*¹⁴ using a fluorescence yield of 0.45. DM: Deutsch–Märk.

between relative and absolute errors in such experiments and estimate theirs to be 2% and 10%, respectively (error bars not shown). We therefore conclude that the quoted errors are, in most cases, representative of the relative errors in the experiments. The uncertainty in the absolute values in Fig. 135.27 would have to be $\sim 20\%$ to make all but a few outlying points consistent with one another, but some of the measurements may have significant systematic errors.

The remainder of this section briefly discusses the general features of these measurements and how they vary with atomic number.

The threshold for K-shell emission is the K-shell binding energy B , or K edge, which is known from measurements and numerical calculations to be 8.98 keV for copper to a precision far greater than any of the other results considered here. K-shell binding energy scales approximately as Z^2 .¹⁷ Above this threshold, the cross section rises sharply, peaks at $\sim 3\times$ the binding energy, then starts to fall. The large number of measurements in this region is in good agreement on the position and shape of the peak, if not on the absolute values. Above ~ 1 MeV, the cross section starts to increase continually from a minimum

that is roughly a factor of 2 below the initial peak for copper. The position of this minimum does not vary significantly with atomic number, and its depth decreases with increasing atomic number as the peak moves up toward it. Eventually it vanishes; for example, gold shows no clear local maximum or minimum in the cross section, showing what could be better described as a point of inflexion. Unfortunately, there are very few measurements in this region, which is the region of particular interest for high-intensity laser–solid experiments; there is only one point between 0.6 and 40 MeV. Therefore, all of the measurements, up to 2 GeV, have been included to see how well expressions interpolate over this region; however, a rigorous analysis of the correlation of the expressions with the measurements has not been carried out since it would be almost meaningless for our purposes.

The expressions—numerical, theoretical, and empirical—all consider the ionization cross section, so a fluorescence yield is required to give the emission cross section. Kahoul *et al.*¹² give a convenient compilation of measurements published before 2011. From these we chose to use 0.45 for three reasons: (1) it is the value from the most-recent measurement given (0.452 ± 0.036); (2) it is the value from the measurement given with the smallest quoted error (0.452 ± 0.003); and (3) it is the highest value since we noted a general tendency for the expressions to lie below the measurements. It should be noted that expressions with parameters obtained by fitting measurements all used fluorescence yields for copper from 0.4 to just under 0.45, so we may slightly overestimate the original fit in some cases. Kahoul *et al.* give five different fits for the fluorescence yield, all of which give adequate agreement with the measurements. The simplest is

$$f_K = 0.985 \frac{(Z/30.896)^{3.847}}{1 + (Z/30.896)^{3.847}}, \quad (2)$$

which gives 0.433 for copper.

K-shell ionization cross sections have been calculated numerically (for example, see Bote *et al.*¹³), but all of these calculations are approximate since an exact model for copper would require solving the full Dirac equation for 30 electrons (one incident electron and 29 electrons in the atom) and this would still neglect collective effects from many atoms. Therefore, these results are not necessarily a better reference than measured values. Also, we have not found a convenient set of tabulated numerical results. We will show Bote *et al.*'s¹⁴ fit to

their numerical results, which has ten fitting parameters determined individually for every element, giving a stated accuracy better than 1% up to the maximum energy considered of 1 GeV.

A plethora of theoretical and empirical expressions exists for the K-shell ionization cross section. To limit the universe of expressions, we did not consider the many nonrelativistic ones that write a factor of $2/m_e v^2$ as $1/E$, leading to a cross section that falls continually with energy above the peak. Such expressions have been used in modeling laser–solid experiments, which would have led to significant errors; $2E/m_e v^2$ exceeds 1.1 at only 34 keV and exceeds 2 at 0.32 MeV. We then considered 12 relativistic expressions,^{14–25} and there are almost certainly more out there. Since this time, a minor modification of Santos *et al.*'s expression²⁵ has been published by Guerra *et al.*²⁶ Only four expressions clearly failed to reproduce the measurements: Jakoby *et al.*'s¹⁶ expression, Tang *et al.*'s¹⁸ expression, Haque *et al.*'s Kolbenstvedt model,²⁰ and Haque *et al.*'s modified Deutsch–Märk model.²³ In the case of Jakoby *et al.*'s expression and Haque *et al.*'s Kolbenstvedt model, this failure appears to be caused, at least in part, by typing errors that we could not resolve. We identified and corrected typing errors in Grynski's relativistic factor²⁷ in Casnati *et al.*'s,¹⁵ Hombourger's,¹⁷ and Gstir *et al.*'s²¹ expressions. Eight models are too many to show conveniently in Fig. 135.27, so we have chosen to plot only six that envelope the range of values given by all eight expressions. The highest values are given by An *et al.*'s²² version of the Deutsch–Märk model,²¹ up to just beyond the dip, and by Santos *et al.*'s²⁵ expression at higher energies. The lowest values are given by Haque *et al.*'s BELI model¹⁹ just above threshold, by Santos *et al.*'s²⁵ expression from there up to the peak, by Haque *et al.*'s XCVTS model²⁴ just beyond the peak, by Bote *et al.*'s¹⁴ expression around the dip, and by Hombourger's¹⁷ expression at higher energies.

The expression of Santos *et al.*²⁵ was used to model our experiments⁷ because it was the first relativistic result we found and they had compared it to measurements for copper, showing adequate agreement; in hindsight we cannot give a rigorous justification for the choice of this expression.

The measurements of Llovet *et al.*¹⁰ represent the most-extensive and accurate single set of measurements of emission cross section from just beyond threshold up to the peak (32 points, roughly a third of all the measurements, from 9.5 keV to 40 keV with a quoted relative error of $\pm 2\%$), so it seems reasonable to use them to determine the most-accurate

expression for ionization cross section in this region, which may be of interest to others. To determine which expression was the most accurate without assuming a value for the fluorescence yield and without being influenced by possible systematic errors in the absolute values of the measurements, we used the gradient of a linear fit to expression versus measurement, the gradient closest to one indicating the most accurate. The expression of Hombourger was the most accurate, with that of Casnati *et al.* coming close. We then found the value of fluorescence yield for these two expressions that gave the best fit to the measurements, obtaining $f_K = 0.488$ for Hombourger and $f_K = 0.455$ for Casnati *et al.*, with Hombourger giving the best fit, as expected. This means that Casnati *et al.* gave the best fit using the fluorescence yield we chose of 0.45. A fluorescence yield of 0.488 is clearly higher than any measured value,¹² indicating that either Hombourger's expression is too low by a factor of $0.488/0.45 = 1.084$, at least for copper, or that Llovet *et al.*'s¹⁰ measurements are systematically high, which would be within their absolute error estimate of $\pm 10\%$. Llovet *et al.*'s measurements are systematically higher than the measurements of Zhou *et al.*,¹¹ but it is not possible to tell whose measurements are more precise. On the other hand, such an increase in Hombourger's expression gives a result at relativistic energies that is closer to all of the other expressions.

Because of the large number and length of the expressions, we have placed them in an appendix, including our corrections to what appear to be typing errors. It is possible, however, to give a simple expression that summarizes them for electron energies E somewhat greater than threshold B (for nonrelativistic B), introducing only three dimensionless parameters f , g , and n that have a limited range of values:

$$\sigma_{\text{ion}} \sim \frac{N_K 100 (1+f)}{\beta^2 B_{\text{keV}}^{1+g}} \ln \left[\left(\frac{\gamma+1}{2} \right)^n \frac{E}{B} \right] \text{ barns}, \quad (3)$$

where N_K is the number of K-shell electrons; β is v/c , where v is the average relative velocity of the fast and K-shell electrons and c is the speed of light; γ is the Lorentz factor of the fast electron; f is between 0 and 1; g is typically 0 or close to 0; and n is 0 or 1. Most models use $n = 0$, while Santos *et al.*,²⁵ Guerra *et al.*²⁶ (not shown), and Bote *et al.*¹⁴ [all based on the results of Scofield²⁸ (not considered)] along with Kolbenstvedt²⁹ (not considered) use $n = 1$. Scofield's expression was not considered because he gave no fitting parameters for copper; Kolbenstvedt's two expressions [his Eq. (11) and the sum of his Eqs. (14) and (15)] were not considered because

they are valid only well above threshold. [Haque *et al.*'s Kolbenstvedt model²⁰ does not have this form, which appears to be a typing error; $T(T+2)$ should replace $(T+2)$ in the log term.] The limited number of measurements above 1 MeV and the significant variations between them mean that a value of n cannot be determined with meaningful accuracy.

In most laser–solid experiments, only the K_α emission is considered, not the K_β emission, so if absolute numbers are required, the K-shell emission cross section must be multiplied by the fraction of K_α emission. Published measurements and numerical calculations of this fraction agree to within a few percent,³⁰ giving 0.880 for copper. Values can also be obtained from the code *FLYCHK*.³¹ This fraction is roughly constant for atomic numbers from 20 to 30, then decreases slowly with atomic number, reaching 0.784 for gold. The copper K_α imagers used in laser–solid experiments image only the $K_{\alpha 1}$ line.⁸ The fraction of K-shell emission in this line has not been as widely considered but can be obtained from *FLYCHK*, which gives 0.591 for copper. It should be noted that these ratios could be higher for many cases of interest as a result of ionization of outer shells caused by target heating.

Before moving on to consider the implication of these results for the interpretation of laser–solid experiments, we will briefly consider the bifurcation in the expressions at relativistic energies ($n = 0$ or 1) out of academic interest.

K-Shell Ionization Cross Section in the Relativistic Limit

The origin of $n = 1$ is a relativistic result for energy transfer to excitation of bound electrons caused by the electric field of a charged particle moving at constant velocity, often called the Bethe term. The origin for $n = 0$ could be the use of the nonrelativistic result $E = p^2/2m_e$ in the Bethe term or the use of the binary collision cross section. Surprisingly, both of these choices differ from the standard expression for fast-electron stopping power^{32,33}

$$\frac{dE}{ds} = - \frac{Z n_a e^4}{4\pi \epsilon_0^2 m_e v^2} \times \left[\ln \left(\sqrt{\frac{\gamma+1}{2}} \frac{E}{I_{\text{ex}}} \right) - \frac{\delta}{2} + \frac{0.909}{\gamma^2} - \frac{0.818}{\gamma} - 0.284 \right], \quad (4)$$

where s is the path length, n_a is the atom number density, e is the electron charge, ϵ_0 is the permittivity of free space, I_{ex} is the mean excitation potential (322 eV for copper), which is usually

determined by fitting measurements, and δ is the density-effect correction, which we will return to later. Bremsstrahlung is not included in this expression. It applies to fast electrons with energy much greater than the binding energy of the electrons contributing to the stopping because they are assumed to be stationary. The connection to K-shell ionization cross section is more obvious if we consider the magnitude of the stopping power caused by only K-shell electrons:

$$\left| \frac{dE}{ds} \right| = -\frac{N_K n_a e^4}{4\pi\epsilon_0^2 m_e v^2} \times \left[\ln \left(\sqrt{\frac{\gamma+1}{2}} \frac{E}{I_K} \right) - \frac{\delta}{2} + \frac{0.909}{\gamma^2} - \frac{0.818}{\gamma} - 0.284 \right] > n_a B \sigma_{\text{ion}}, \quad (5)$$

where I_K is the mean excitation potential for K-shell electrons, which exceeds their binding energy;³² for example, for hydrogen the mean excitation potential is 19.2 eV, whereas the binding energy is 13.6 eV. The magnitude of the stopping power must be greater than $n_a B \sigma_{\text{ion}}$ because B is the minimum energy exchange in a K-shell ionization event and energy can be lost to K-shell electrons without ionizing them. This indicates that n should be $1/2$, not 0 or 1—a value that has not been used in any expression we have encountered. The origin of this $n = 1/2$ is a combination of binary collisions for large energy transfers and the Bethe term for small energy transfers.

The density-effect correction represents a reduction in stopping power caused by shielding of the fast electron's charge by surrounding electrons, which is not considered in the Bethe term. It increases with density of the surrounding electrons and with fast-electron energy, occurring only above a threshold energy in insulators. It has not been included in any of the expressions considered here, although Santos *et al.* state that it should be included at energies greater than a GeV and Scofield,²⁸ who did not consider copper, did include it. In copper, the reduction in total stopping power exceeds 10% above roughly 10 MeV (Refs. 32 and 33), indicating that the density effect should be considered at energies considerably less than a GeV, and this energy will decrease with increasing atomic number. The general expression is complex, but it has a simple limiting form for strongly relativistic electrons:

$$\frac{\delta}{2} \rightarrow \ln \left(\frac{\gamma \hbar \omega_p}{I_{\text{ex}}} \right) - \frac{\beta^2}{2}, \quad \beta \rightarrow 1, \quad (6)$$

where $\hbar \omega_p$ is the plasmon energy calculated from total electron density (58.3 eV for copper). Equation (6) is within 10% of a more-accurate calculation for copper^{32,33} above roughly 30 MeV; at lower energies it is an underestimate.

This implies that the rate of increase in the K-shell ionization cross section with energy should noticeably decrease at strongly relativistic energies. If the density-effect correction is not included in the expressions of Santos *et al.*²⁵ and Guerra *et al.*,²⁶ the inequality in Eq. (5) will not hold in the strongly relativistic limit (to this extent they are correct to state that the density effect should be included above 1 GeV). For expressions using $n = 0$, including the density effect will give a cross section that becomes independent of energy at strongly relativistic values, indicating that $n = 0$ is not a physically correct choice. Scofield²⁸ did find that the density effect led to the cross section becoming independent of energy, but this appears to be a mistake in using δ in place of $\delta/2$ combined with his use of $n = 1$. The maximum cross section he gives is lower than values that have been measured at high energies and no saturation in any K_α cross section has yet been reported.

Calculations and fitting formulas of the density-effect correction are readily available.^{32–34} We found that the total stopping power of copper^{32,33} was reproduced to within 1% by using

$$\frac{\delta}{2} = \ln \left[1 + (\gamma - 1) \frac{\hbar \omega_p}{I_{\text{ex}}} \exp(-0.5) \right], \quad (7)$$

which is zero at zero energy and tends to Eq. (6) in the relativistic limit, but does not fit at intermediate energies; however, here the density-effect correction makes a negligible contribution to the stopping power and the same would be expected for the K-shell ionization cross section. This will also work well for higher- Z metals; we have found that it works better for molybdenum, but not insulators, where there is a threshold energy for the density effect to occur.

There is a potential complication when considering the inclusion of the density effect: the nanometer-thick films used in many of the measurements could suppress it because it is a collective effect that requires a minimum amount of material. For a strongly relativistic electron, the relevant length scale should be c/ω_p , which is 3.4 nm for copper, so this is a concern. Evaluating the density effect in this case will require numerical calculations. We therefore conclude that the correct value of n

appears to be 1/2 and that the density-effect correction should be included for copper at fast-electron energies above 10 MeV and at lower energies for higher atomic numbers.

Finally, it should be noted that these considerations as to which value of n is physically correct and the need to include the density-effect correction strictly apply only to physics-based expressions, such as those of Santos *et al.*²⁵ and Guerra *et al.*²⁶ Expressions with free parameters used to fit measurements could still give adequate fits over any energy range of interest, whatever value of n is assumed and without including the density effect, although a better physical basis for a fitting function should allow one to obtain a better fit. If an expression with free parameters is modified, the free parameters should be redetermined.

K-Shell Emission as a Fast-Electron Diagnostic in Laser–Solid Experiments

Some of the implications of these results for K-shell emission diagnostics in laser–solid experiments will now be considered, the first being the choice of a K-shell emitter based on K-shell yield.

Using $\sigma_{\text{ion}} \propto Z^{-2}$ ¹⁷ and Eq. (2) for the fluorescence yield, we find that there is a maximum in the K-shell emission cross section at an atomic number close to 21, which is scandium. Considering the atomic number density of solids in this region, the maximum macroscopic cross section should belong to titanium (22), which has been used in high-intensity laser–solid experiments almost as frequently as copper. Considering that the K-shell emission self-absorption depth is roughly proportional to the atomic number, increasing the thickness of the layer from which emission can be obtained and consequently total yield, we find that maximum yield occurs near 29, which is copper. This provides a further motivation for concentrating on copper, although, given the approximations made, nickel or zinc could give a higher yield. The available measurements do not allow one to more precisely determine the maximum emission cross section and maximum yield.

For time-resolved measurements, the key parameter is an emission rate of $n_a \sigma v$; the results given in Fig. 135.27 multiplied by velocity are shown in Fig. 135.28. The emission rate has no initial peak and is almost independent of energy over the range of interest. This means that the K_α -emission rate is, to a good approximation, proportional to the number of fast electrons, provided that the mean energy is much greater than the binding energy. Our results,⁷ which did not depend on

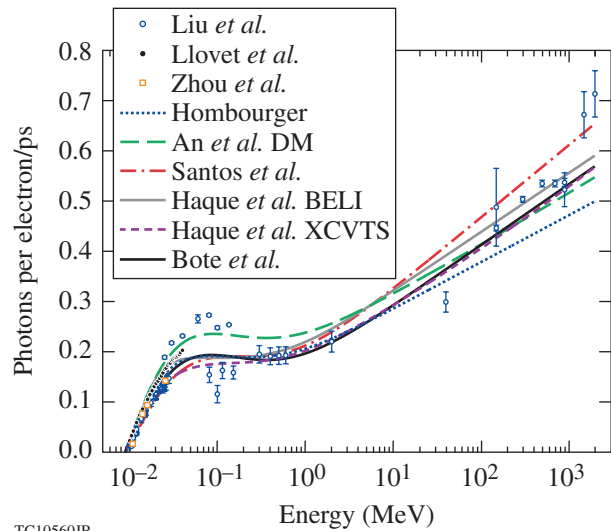


Figure 135.28

Same as Fig. 135.27 but multiplied by the electron velocity to give the emission rate in copper.

absolute values, were found to be insensitive to the expression used and to some accidental variations of individual terms in the expression of Santos *et al.*²⁵ by a factor of 2 because all of these expressions give an approximately constant emission rate at the relevant energies. This would not have been the case if the mean fast-electron energy was not much greater than the binding energy; just above the binding energy, the emission rate increases significantly with energy and the different expressions would give noticeably different results.

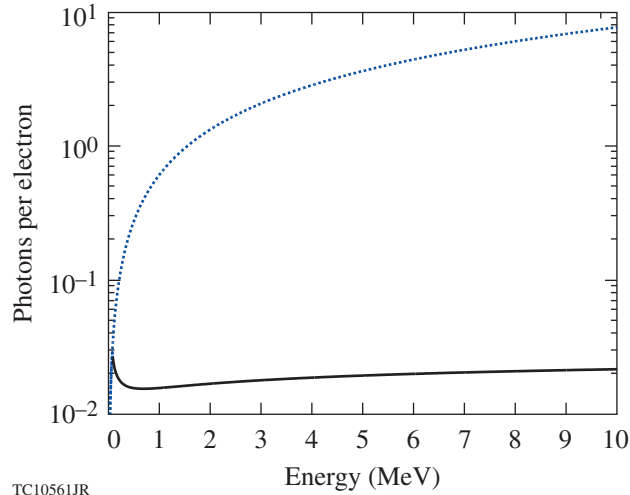
The most important parameter in determining the sensitivity of K-shell emission diagnostics to electron energy is the yield per electron Y , so we will now calculate this for two cases of particular interest to laser–solid experiments.

For an isolated copper foil, the vast majority of the electrons will be confined to the foil by the electrostatic field they generate, so K-shell emission yield will be determined by the emission rate times the stopping time. Considering only stopping resulting from collisions given by Eq. (4), the yield is

$$Y = \int_B^E \frac{n_a \sigma_K}{|dE/ds|} dE. \quad (8)$$

To illustrate this result for copper, we used only the BELI model of Haque *et al.*¹⁹ since it lies roughly in the middle of the others over the energy range of interest. This yield is given by the

upper line in Fig. 135.29; it increases continually with energy, tending to a linear increase at high energies. Bremsstrahlung would lead to the yield flattening out by about 60 MeV, when it becomes the dominate energy-loss mechanism in copper.³²



TC10561JR

Figure 135.29

K-shell yield per electron including collisional stopping in solid, un-ionized copper for electrons that stop in the copper (dotted blue line) and electrons that travel a maximum distance of 20 μm (solid black line).

Equations (3) and (8) indicate that ZBY/f_K as a function of E/B should be weakly dependent on material, while bremsstrahlung is negligible, so this result can be readily scaled to any material of interest. Bremsstrahlung will lead to the yield flattening out at lower energies for higher atomic numbers.

Most K-shell emission experiments use a thin layer buried within a thick target. For electrons that maintain a constant velocity and travel a distance s , the yield is simply $n_a \sigma_K s$; therefore, its variation with energy is the same as that for the macroscopic cross section given in Fig. 135.27. The lower line in Fig. 135.29 gives the yield for electrons traveling a maximum distance of 20 μm , a typical upper value for the thickness of a copper fluor layer since it is roughly the attenuation depth of the K-shell emission. This gives a yield that is practically independent of energy from 0.7 to 10 MeV. Below this there is a narrow peak, where the yield increases by a factor of 1.9; then below 60 keV, the yield rapidly becomes negligible. In practice, the yield per electron from a 20- μm copper layer would lie between the two curves in Fig. 135.29 because the distance traveled by an electron going through the layer at an angle θ to the normal will be $20/\cos\theta$ μm and angular scattering will increase the average path length,³⁵ more so for

lower-energy electrons. Therefore, to a first approximation, copper K-shell emission from a thin layer in a thick target is proportional to the number of electrons above roughly 60 keV that reach it, provided that the majority of electrons reaching it exceed this energy.

An important general feature to note from Fig. 135.29 is that collisions significantly suppress the K-shell emission yield of electrons with an energy up to roughly $6\times$ the threshold energy; therefore, the effective detection threshold is significantly higher than might be expected. The physical reason for this is that electrons just above threshold are far more likely to lose their energy colliding with one of the other electrons in the material than to cause K-shell emission. Another important feature is that the local maximum in the K-shell emission cross section does not lead to the emission being particularly sensitive to a narrow range of fast-electron energies, as is often assumed. For mean energies well above the effective threshold, K-shell emission, either time resolved from an isolated thin foil or time integrated from a thin foil buried in a thick target, is most sensitive to the number of fast electrons and not sensitive to their energy. The energy distribution can be inferred from the variation in signal with time or depth, provided the energy dependence of stopping time or distance is known. The only significant difference between the expressions we have considered will be in determining the absolute number of fast electrons. For mean energies that are not much greater than threshold, K-shell emission will be dominated by the higher-energy electrons in the distribution and interpretation of the results will be sensitive to the shape of the cross section near threshold, where the expressions we have considered are noticeably different.

Another important factor when evaluating absolute yields in experiments is the opacity of the target, which can change significantly as it ionizes, but this will not be considered here.

We will next examine how accurate it is to assume that K-shell emission measurements in laser–solid experiments are due entirely to fast electrons.

Other Sources of K-Shell Emission

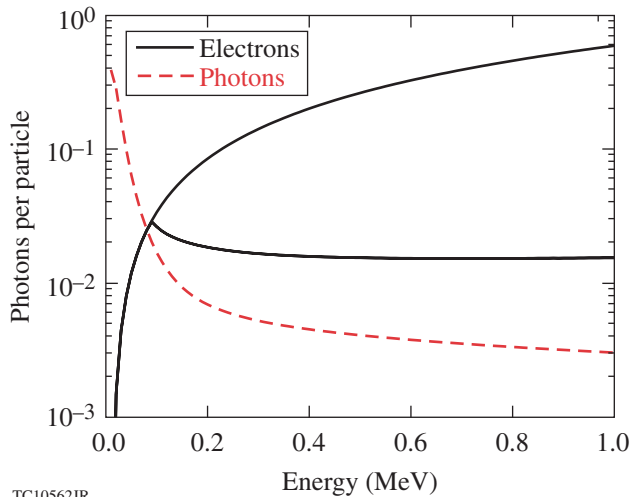
An essential requirement when using K-shell emission as a fast-electron diagnostic is that fast electrons be the primary source of the emission, but photons and ions can also cause K-shell emission and are also produced in laser–solid interactions, so we will briefly consider the yields from these other potential sources of K-shell emission.

1. Photons

To estimate the yield from photons, we considered only photons below the threshold for pair production (1.022 MeV) where absorption is caused only by photoionization. For the fraction of K-shell photoionizations in copper, we used 0.8796, as used in the EGS Monte Carlo code;³⁶ therefore, we need to calculate only $0.8796 \times$ the number of photons absorbed in the copper. To do this, we assumed an isotropic photon source and averaged exponential attenuation over all straight-line trajectories through a sheet of thickness s , obtaining

$$Y = 0.396 \left[1 - \exp\left(-\frac{s}{l_{\text{ph}}}\right) + \frac{s}{l_{\text{ph}}} E_1\left(\frac{s}{l_{\text{ph}}}\right) \right], \quad (9)$$

where E_1 is the exponential integral and l_{ph} is photon attenuation depth, obtained from XCOM,³⁷ excluding photon scattering, which makes only a small contribution to photon attenuation. This result for a 20- μm copper layer is plotted in Fig. 135.30 along with the previous results for electron yields.



TC10562JR

Figure 135.30
K-shell yield per photon for an isotropic distribution of photons incident on a 20- μm copper layer and the yields per electron from Fig. 135.29.

The yield for photons has a maximum at threshold and decays continually with energy, whereas the yield for electrons is zero at threshold and increases continually with energy. This indicates that, for copper, photons less than 70 keV are of particular concern because they could cause more K-shell emission than electrons with only a fraction of the energy of the electrons. This justifies the neglect of photons above 1 MeV, although the pairs produced by higher-energy photons would contribute to K-shell emission (not considered here).

Three principle sources of photons in laser-solid experiments could cause K-shell emission: bremsstrahlung from fast electrons in the target, emission from the laser-heated plasma on the front surface, and line emission from higher- Z elements, if present.

Bremsstrahlung will turn a fraction of the fast-electron energy into photons with a comparable energy distribution. This fraction, the radiation yield, increases with electron energy and the atomic number of the target.³² Radiation yield becomes significant only for electron energies greater than 1 MeV, where electrons always have a far greater K-shell yield than photons, so in most cases bremsstrahlung will not make a significant contribution to the total yield, with the possible exception of very high- Z targets. Even though the *total* yield from bremsstrahlung photons should be negligible, the K-shell emission from a layer at a large-enough depth may be dominated by bremsstrahlung photons because the attenuation depth of photons is larger than the mean free path of electrons at the same energy. In other words, the fraction of the fast-electron energy distribution converted into photons would be expected to propagate farther into a target than the fast electrons.

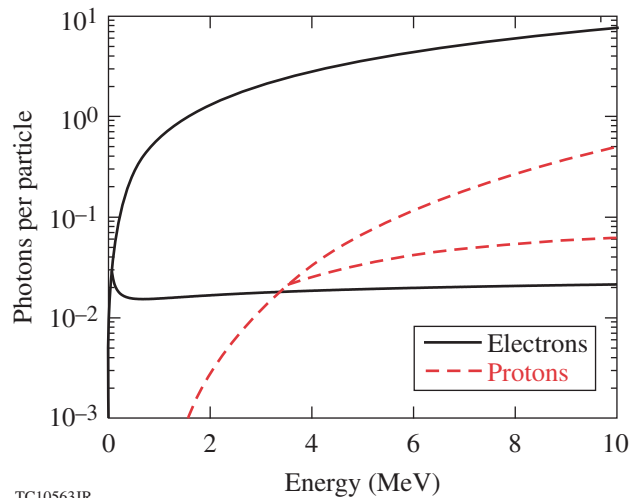
The laser-driven plasma could emit a significant number of photons just above the K edge. Unfortunately, it is not straightforward to estimate this emission since the systems of interest are usually far from equilibrium; therefore we cannot, in general, easily rule out a significant contribution to K-shell emission from this source. A good means of quantifying this in experiments would be to measure the x-ray emission in the relevant range from the front of the target.

If elements with a higher Z than the K-shell emitting layer are used in targets (for example, to give two emitters in one target), the line emission must be carefully considered; a non-negligible fraction of the emission from the higher- Z layer could cause emission from the lower- Z layer. This must be considered for each individual target design.

2. Protons

For ions we will consider only protons since they are always present; because of impurities, protons are the ions that are most efficiently accelerated in laser-plasma interactions and they have, by far, the lowest stopping power of all ions.

To estimate the yield from protons in copper, we used the K-shell ionization cross section from Kahoul *et al.*³⁸ (given in the appendix), who fitted a compilation of experimental results between 80 keV and 13 MeV, and we used the proton-stopping



TC10563JR

Figure 135.31

Same as Fig. 135.29 but for protons as well as electrons.

power given by PSTAR.³⁹ The result, seen in Fig. 135.31, is combined with our previous results for the yield from electrons.

Proton and electron energies have been found to be strongly correlated to one another in laser–solid interactions,³ so it is reasonable to compare the yields at the same energies. For a thin, isolated target where the majority of the electrons are expected to recirculate and any protons are expected to go through the target, K-shell emission yield per proton will always be lower than that per electron. For a thin layer in a thick target, the yield per proton can exceed the yield per electron; for a 20- μm copper layer this occurs above 3.4 MeV because the cross section for protons then exceeds that for electrons. Despite this, the total yield from protons would be expected to be lower than that from electrons because the fraction of laser energy transferred to protons entering the target has been found to be lower than that for electrons, for parameters of interest. Emission from protons accelerated into the target may not be entirely negligible, however, particularly at the higher intensities used, and there could be regions in the target where the number of protons equals or exceeds the number of electrons, so it would be worth considering in a more-detailed analysis.

Conclusions

Nine expressions for K-shell ionization cross sections^{14,15,17,19,21,22,24–26} have been identified that, based on published measurements for copper,^{9–11} appear to be adequate for modeling copper K-shell emission diagnostics used in high-intensity laser–solid experiments. For the fluorescence yield required to convert the K-shell ionization cross section to the K-shell emission cross section, a useful summary of measure-

ments and fitting formulas has been given by Kahoul *et al.*¹² For copper we chose 0.45 and, if required, we would consider the uncertainty in this value to be ± 0.01 . For the fraction of K-shell emission in the K_{α} line, published measurements and numerical calculations^{30,31} are in good agreement, giving 0.880; a reasonable estimate of the uncertainty in this value would be ± 0.01 . We were unable to narrow down the field because very little attention has been paid to energies from 0.1 to 10 MeV. Instead, past attention has concentrated on the behavior of ionization cross sections near threshold. In this region, the expression given by Hombourger¹⁸ with a fluorescence yield of 0.488 gave the best fit to measurements. The only models that are clearly inadequate are the nonrelativistic ones that use a factor of $1/E$ in place of $2/m_e v^2$.

Should an estimate of the uncertainty in the K-shell emission cross section be required, we suggest a conservative value of $\pm 20\%$. Alternatively, a number of these expressions that give upper and lower bounds on the cross section could be used. We found that six expressions were required to give upper and lower bounds over the full range of energies, at least for copper, but for most applications four expressions should be sufficient: Santos *et al.*²⁵ (or Guerra *et al.*²⁶), An *et al.*,²² Hombourger,¹⁸ and Bote *et al.*¹⁴

In examining these models we identified an unresolved issue regarding the energy dependence of the ionization cross section at relativistic energies: the factor n in Eq. (3), where either 0 or 1 is used. By comparison with the standard result for fast-electron stopping power,³² we found that $n = 1/2$ appears to be the correct choice. Furthermore, we found for copper that the density-effect correction should be considered above 10 MeV, and this energy will decrease with an increasing atomic number. The available measurements at strongly relativistic energies are insufficient to indicate which form is correct and how the density-effect correction should be included. In order to provide an adequate fit to cross sections for energies of current interest, these are not important issues but are interesting physics issues for future work in this area.

Using these results and the standard expression for electron stopping power, it was found that the effective detection threshold of K-shell emission diagnostics is roughly $6\times$ higher than the threshold energy for causing K-shell emission. Both the K_{α} -emission rate, as used in our experiments,⁷ and the total K_{α} emission from typical buried layer experiments are approximately proportional to the number of electrons above this threshold and are not sensitive to the electron energy, provided that the majority of fast electrons are above the

effective detection threshold. Near the detection threshold, K_{α} emission is far more sensitive to electrons with higher energies, and current uncertainties in the cross section will lead to significant uncertainties in interpreting measurements. The local maximum in the K_{α} -emission cross section does not lead to K_{α} emission being particularly sensitive to a narrow range of electron energies, as is often assumed.

K-shell emission caused by photons and protons was briefly considered. Photons from the laser-heated plasma and higher-Z layers could make a significant contribution in some experiments and deserves careful consideration. Protons accelerated into the target should not make a significant contribution because of their smaller number, but if significant numbers of protons above 3 MeV are accelerated into the target, they should be considered in a more-detailed modeling.

Appendix A: Expressions for K-Shell Ionization Cross Sections

For the incident electron we use E for kinetic energy, v for velocity, β for v/c , where c is the speed of light, and γ for the Lorentz factor ($1 + E/m_e c^2$), where m_e is the electron mass. For the K-shell electrons we use B for binding energy, B_{keV} when it is expressed in keV (SI units are used unless specified), and N_K for number (2 for all cases of interest). The material is indicated by its atomic number Z . Three expressions use Rydberg energy R (13.606 eV). Two dimensionless parameters are used in most expressions:

$$U = \frac{E}{B}, \quad (\text{A1})$$

often called the overpotential, and

$$J = \frac{m_e c^2}{B} \quad (\text{A2})$$

(56.9 for copper), which appears naturally when writing relativistic expressions in terms of U . A number of the expressions use Grysinski's relativistic factor²⁷ written as

$$G = \frac{1+2J}{U+2J} \left(\frac{U+J}{1+J} \right)^2 \times \left[\frac{(1+U)(U+2J)(1+J)^2}{J^2(1+2J)+U(U+2J)(1+J)^2} \right]^{1.5}, \quad (\text{A3})$$

which is intended to convert a nonrelativistic expression for energy exchange in a binary collision between electrons with kinetic energies E and B to a relativistically correct expression. This always appears as G/E , so we introduce the parameter

$$G' = \frac{G}{2(\gamma-1)} = \frac{JG}{2U}. \quad (\text{A4})$$

The reason for this choice, and the effect of this complex-looking term, can be easily illustrated by considering a nonrelativistic binding energy $J \gg 1$, valid for most cases of interest,

$$G' \approx \frac{1}{\beta^2}, \quad B \ll m_e c^2, \quad (\text{A5})$$

so Grysinski's relativistic factor essentially replaces the $1/E$ in nonrelativistic expressions with $2/m_e v^2$. We believe that a number of the expressions have typing errors in this factor.^{15,17,21}

Casnati *et al.*'s¹⁵ expression for any element is

$$\begin{aligned} \sigma_0 &= \frac{N_K 187}{B_{\text{keV}}^{1.0318}} \text{ barns}, \\ f &= -\frac{0.316}{U} + \frac{0.1135}{U^2}, \\ \sigma_{\text{ion}} &= \sigma_0 G' \left(\frac{R}{B} \right)^f \exp \left(-\frac{1.736}{U} + \frac{0.317}{U^2} \right) \ln U. \end{aligned} \quad (\text{A6})$$

Tang *et al.*¹⁸ used this expression and obtained different fitting parameters: 137 and 1.0514 in σ_0 , -0.4935 and 0.3529 in f , and -1.227 and -0.2791 in the exponential. Note that a_0 in their expression should be a_0^2 and that their coefficients C_{1-3} have the wrong sign, or, equivalently, it should be $-C_u$ or (E_k/R_y) in place of (R_y/E_k) .

Jakoby *et al.*'s¹⁶ expression and Haque *et al.*'s²⁰ Kolbenstvedt expression, as printed, do not reproduce the published figures. Even after correcting a number of obvious typing errors and experimenting with likely looking variants, we could not obtain sensible results; therefore we have not reproduced them here.

Hombourger's¹⁷ expression for any element is

$$\begin{aligned}\sigma_0 &= \frac{N_K 175}{B_{\text{keV}}^{1.0305}} \text{ barns}, \\ f &= -\frac{0.316}{U} + \frac{0.1545}{U^2}, \\ \sigma_{\text{ion}} &= \sigma_0 G' \left(\frac{R}{B} \right)^f \left(1 - \frac{1.335}{U} + \frac{0.6006}{U^2} \right) \ln U.\end{aligned}\quad (\text{A7})$$

We suggest using $N_K 190 / B_{\text{keV}}^{1.0305}$ for σ_0 based on fitting this expression to the measurements of Llovet *et al.*¹⁰ and measurements of the fluorescence yield for copper¹² that indicate a value of 0.45.

Haque *et al.*'s¹⁹ BELI expression for any element is

$$\begin{aligned}\sigma_0 &= \frac{N_K 205}{B_{\text{keV}}} \text{ barns}, \\ \sigma_{\text{ion}} &= \sigma_0 G' \left[1 + 3 \left(\frac{1 - N_K / Z}{U} \right)^{1.27} \right] \\ &\quad \times \left[\ln(U) + \sum_{n=1}^5 b_n \left(1 - \frac{1}{U} \right)^n \right],\end{aligned}\quad (\text{A8})$$

where b_n is $-0.971, 0.381, 0.0952, -0.0476,$ and -0.190 . The term in brackets following Grynski's relativistic factor represents shielding of the K-shell electrons by the remaining electrons in the atom.

A number of expressions have been based on the Deutsch-Märk model. For these we use

$$\sigma_0 = 1.72 \times 10^{-3} f_H r_K^2, \quad (\text{A9})$$

where $f_H = 0.553$ for hydrogen and $= 1$ otherwise and r_K is the radius of maximum areal density, tabulated (in units of the Bohr radius 5.2918×10^{-11} m) by Desclaux,⁴⁰ which is 1.807×10^{-12} m for copper. The most-recent version we found from the originators of the model is Gstir *et al.*:²¹

$$\begin{aligned}\sigma_{\text{ion}} &= \sigma_0 \left(1 + \frac{2U^{0.25}}{J^2} \right) G' \left(\frac{U-1}{U+1} \right)^{1.06} \\ &\quad \times \left(1.353 - \frac{0.55}{U} \right) \ln(2.7 + \sqrt{U-1}).\end{aligned}\quad (\text{A10})$$

The first term in parentheses is a modification to Grynski's relativistic factor. An *et al.*²² have since determined the fitting parameters including subsequent measurements:

$$\begin{aligned}\sigma_{\text{ion}} &= \sigma_0 \left(1 + \frac{2U^{0.25}}{J^2} \right) G' \left(\frac{U-1}{U+1} \right)^{0.95} \\ &\quad \times \left(1.4 - \frac{0.475}{U} \right) \ln(2.7 + \sqrt{U-1}).\end{aligned}\quad (\text{A11})$$

Haque *et al.*²³ give a significantly modified version

$$\begin{aligned}\sigma_{\text{ion}} &= \sigma_0 \frac{1 + 1.5J}{1.2J} \left(1 + \frac{1.5U^{0.055}}{J} \right) \\ &\quad \times G' \left(1 + 6.75 \frac{1 - N_K / Z}{Z^{0.5} U} \right)^{0.85} \\ &\quad \times \left[0.86 - \frac{0.63}{1 + (U/3.76)^{2.08}} \right] \ln(1.01U).\end{aligned}\quad (\text{A12})$$

The first two terms are modifications to Grynski's relativistic factor, and the term following it represents shielding of the K-shell electrons by the remaining electrons in the atom. We believe there may be typing errors in this expression.

Haque *et al.*'s²⁴ XCVTS expression is

$$\begin{aligned}\sigma_0 &= \frac{N_K 4.5 \times 10^6 B_{\text{keV}}}{Z^{4.35}} \text{ barns}, \\ \sigma_{\text{ion}} &= \sigma_0 \left(\frac{U+J}{1+J} \right)^{0.02} \left(1 - \frac{0.22U^{0.27}}{J^2} \right) \\ &\quad \times G' \left(1 + 0.01 \frac{Z - N_K}{U} \right) \ln U.\end{aligned}\quad (\text{A13})$$

The first term is a modification to Grynski's relativistic factor. The next term in parentheses, introduced to prevent the expression from increasing without limit, cannot be correct for strongly relativistic energies since it will eventually lead to a negative cross section; there is also nothing to indicate that the cross section does not increase continually with energy. The term after Grynski's relativistic factor represents shielding of the K-shell electrons by the remaining electrons in the atom.

Bote *et al.*'s¹⁴ fit to their numerical results for copper is

$$U \leq 16,$$

$$\sigma_0 = 351.9 \text{ barns},$$

$$\sigma_{\text{ion}} = \sigma_0 \frac{U-1}{U^2} \times \left[3 + 0.05003U - \frac{3.48}{1+U} + \frac{3.339}{(1+U)^3} - \frac{3.683}{(1+U)^5} \right]^2, \quad (\text{A14})$$

$$U > 16,$$

$$\sigma_0 = \frac{22.84U}{U+0.765} \frac{1}{\beta^2} \text{ barns},$$

$$x = \sqrt{\gamma^2 - 1},$$

$$\sigma_{\text{ion}} = \sigma_0 \left\{ \left[\ln(x^2) - \beta^2 \right] \left(1 + \frac{0.3024}{x} \right) + 6.261 - \frac{1.024}{\sqrt{\gamma}} + \frac{0.4543}{x} \right\}.$$

The fitting parameters for other elements can be found in Bote *et al.*'s paper. Note that they calculate the binding energy of copper to be 8.95 keV, not 8.98 keV.

For Santos *et al.*'s²⁵ and Guerra *et al.*'s²⁶ expressions, we use

$$\sigma_0 = \frac{N_K 255}{B_{\text{keV}}} \text{ barns}, \quad (\text{A15})$$

$$\sigma_B = \sigma_0 \left\{ \frac{1}{2} \left[\ln \left(\frac{\gamma+1}{2} U \right) - \beta^2 \right] \left(1 - \frac{1}{U^2} \right) + 1 - \frac{1}{U} + \left(\frac{2}{\gamma+1} \right)^2 \left[\frac{U-1}{2J^2} - (2\gamma-1) \frac{\ln U}{1+U} \right] \right\}.$$

We believe that the density-effect correction $(-\delta/2)$ should be inserted in the first set of square brackets. This is divided by a term of the form β^2 , which could be interpreted as the mean-

squared relative velocity of the incident and K-shell electrons. Santos *et al.*'s²⁵ give

$$\sigma_{\text{ion}} = \frac{\sigma_B}{2} \left(\frac{1}{\beta^2} + \frac{1}{\beta^2 + \beta_B^2 + \beta_K^2} \right), \quad (\text{A16})$$

where

$$\beta_x^2 = 1 - \frac{1}{(1 + x/m_e c^2)^2}, \quad (\text{A17})$$

where x is an energy and K is the mean kinetic energy of the K-shell electrons, tabulated in Santo *et al.*'s paper (11.32 keV for copper). Guerra *et al.* give

$$\sigma_{\text{ion}} = \frac{\sigma_B}{\beta^2 + (0.126 - 0.213Z + 0.195Z^2)(2R/B)\beta_B^2}. \quad (\text{A18})$$

Kahoul *et al.*'s³⁸ expression for copper K-shell ionization by protons is

$$x = \ln \left(\frac{E_{\text{MeV}}}{16.489} \right), \quad (\text{A19})$$

$$\sigma_{\text{ion}} = \frac{\exp(11.292 + 0.192x - 0.371x^2 + 0.028x^3)}{80.6404} \text{ barns}.$$

The fitting parameters for other elements can be found in Kahoul *et al.*'s paper.

Appendix B: A Proposed Fit to the K-Shell Emission Cross Section of Copper

Our objective was never to develop our own expression for the K-shell emission cross section but to find a simple expression that we could plug into our calculations; this is most likely the reader's objective, so it appears to be something of a disservice to end with a long list of complex expressions and no clear recommendation. Therefore, we will propose a simple expression for the K-shell emission cross section of copper that gives the best fit to the measurements and that in the limit of strongly relativistic energies has the form indicated by the fast-electron stopping power. Since 77% of the measurements are in the region from threshold to peak, the best fit to them is largely determined by the form of the expression in this region.

A simple expression that reproduces all of the general features and has the desired limiting form is

$$f_0 = \frac{\sigma_0}{\beta^2} \left\{ \ln \left[\left(\frac{\gamma + 1}{\gamma_B + 1} \right)^{1/2} U \right] - \frac{\delta - \delta_B}{2} \right\}, \quad (\text{B1})$$

where the subscript B indicates quantities evaluated at the binding energy B , rather than the fast-electron kinetic energy E , to give an expression that is identically zero at threshold. An equally valid approach would be to multiply by a function that is zero at threshold and tends to a constant at large energies.

The density-effect correction δ could be calculated either numerically, from tabulated values, or from a fitting formula. An approach that may provide the best means to fit data would be to use a fitting formula and redetermine its parameters by fitting the data. For a number of applications it could be ignored. For simplicity we used Eq. (7), which is intended to have the right form in the strongly relativistic limit and not to cause significant errors at lower energies; it is not a fitting formula. At energies of the order of 1 MeV, it is an underestimate. It will not work for nonconductors and will not work well for lower Z than copper.

Equation (B1) does not give a good fit to the measurements. Since Hombourger's expression gave the best fit to Llovet *et al.*'s data, we tried multiplying f_0 by

$$f_1 = 1 + \sum_{n=1}^N \frac{a_n}{U^n}. \quad (\text{B2})$$

$N = 1$ gave a good fit to Llovet *et al.*'s data and the fit did not improve significantly until $N = 4$, which gave a value of σ_0 that appeared too low (16.95 barns). We also used $N = 1$ to fit all of the measurements and obtained very similar results. The resulting expression for the K-shell emission cross section of copper is

$$\sigma_K = \left(1 - \frac{0.2824}{U} \right) \frac{20.95}{\beta^2} \times \ln \left[\left(\frac{U + 113.8}{114.8} \right)^{1/2} \frac{57.0098U}{56.9 + 0.1098U} \right] \text{ barns}. \quad (\text{B3})$$

The resulting macroscopic cross section is plotted along with the measurements in Fig. 135.32, where we have included the $\pm 10\%$ absolute error quoted by Llovet *et al.*,¹⁰ imposed a minimum error of $\pm 10\%$ on the measurements given by Liu *et al.*,⁹ and plotted our fit at the $\pm 10\%$ levels. We have not plotted the other expressions in order to emphasize a comparison with the

measurements and avoid too many lines. Our proposed fit is in good agreement with the measurements up to and just beyond the peak but agrees only with subsets of the measurements compiled by Liu *et al.*⁹ at higher energies, even considering variations of $\pm 10\%$, which is also true of all the other expressions. Compared to the other expressions, it lies roughly in the middle of them up to just above the peak, where it clearly gives the best fit to the measurements, gives the highest values near the dip, lies within their range of values between roughly 50 MeV and 2 GeV, and gives the lowest values at higher energies.

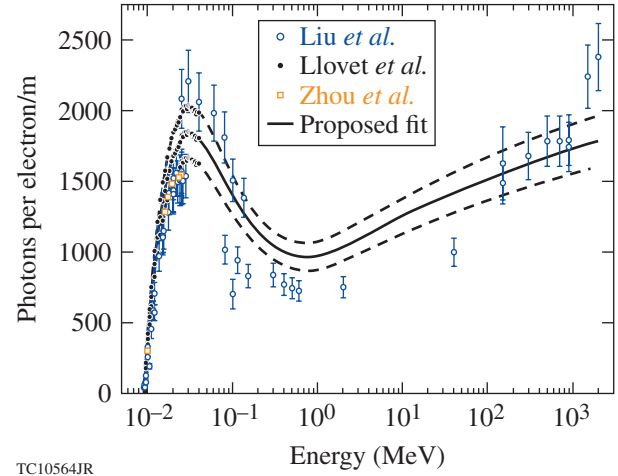


Figure 135.32

Macroscopic K-shell emission cross sections for solid copper. Circles are measurements compiled by Liu *et al.*⁹ with a minimum error of $\pm 10\%$ imposed. Dots joined by a solid line are the measurements of Llovet *et al.*,¹⁰ the dots on the dashed lines are these values at $\pm 10\%$ —their quoted absolute error. Squares are the measurements of Zhou *et al.*¹¹ The solid line is our proposed fit; dashed lines are the fit at $\pm 10\%$.

This approach is good only for fitting data from threshold to peak; f_1 in all the fits was close to one beyond the peak. Further factors should be added that can adjust the depth of the dip and the value of σ_0 in the strongly relativistic limit; it does appear that the dip should be lowered. We have not considered this further because there are only a limited number of measurements with significant differences between them in this region.

ACKNOWLEDGMENT

This work has been supported by the U.S. Department of Energy under Cooperative Agreement Nos. DE-FC02-04ER54789, Fusion Science Center supported by the Office of Fusion Energy Sciences, and DE-FC52-08NA28302 Office of Inertial Confinement Fusion, the New York State Energy Research Development Authority, and the University of Rochester. The support of DOE does not constitute an endorsement by DOE of the views expressed in this article.

REFERENCES

1. M. Tabak *et al.*, Phys. Plasmas **1**, 1626 (1994).
2. S. Gus'kov *et al.*, Phys. Rev. Lett. **109**, 255004 (2012).
3. J. T. Mendonça, J. R. Davies, and M. Eloy, Meas. Sci. Technol. **12**, 1801 (2001).
4. J. R. Davies, Laser Part. Beams **20**, 243 (2002).
5. S. P. Hatchett, C. G. Brown, T. E. Cowan, E. A. Henry, J. S. Johnson, M. H. Key, J. A. Koch, A. B. Langdon, B. F. Lasinski, R. W. Lee, A. J. MacKinnon, D. M. Pennington, M. D. Perry, T. W. Phillips, M. Roth, T. C. Sangster, M. S. Singh, R. A. Snavely, M. A. Stoyer, S. C. Wilks, and K. Yasuike, Phys. Plasmas **7**, 2076 (2000).
6. M. I. K. Santala *et al.*, Phys. Rev. Lett. **84**, 1459 (2000).
7. P. M. Nilson, J. R. Davies, W. Theobald, P. A. Jaanimagi, C. Mileham, R. K. Jungquist, C. Stoeckl, I. A. Begishev, A. A. Solodov, J. F. Myatt, J. D. Zuegel, T. C. Sangster, R. Betti, and D. D. Meyerhofer, Phys. Rev. Lett. **108**, 085002 (2012).
8. K. B. Wharton *et al.*, Phys. Rev. Lett. **81**, 822 (1998); R. B. Stephens *et al.*, Phys. Rev. E **69**, 066414 (2004); K. L. Lancaster, J. S. Green, D. S. Hey, K. U. Akli, J. R. Davies, R. J. Clarke, R. R. Freeman, H. Habara, M. H. Key, R. Kodama, K. Krushelnick, C. D. Murphy, M. Nakatsutsumi, P. Simpson, R. Stephens, C. Stoeckl, T. Yabuuchi, M. Zepf, and P. A. Norreys, Phys. Rev. Lett. **98**, 125002 (2007); J. S. Green *et al.*, Phys. Rev. Lett. **100**, 015003 (2008).
9. M. Liu *et al.*, At. Data Nucl. Data Tables **76**, 213 (2000).
10. X. Llovet, C. Merlet, and F. Salvat, J. Phys. B **33**, 3761 (2000).
11. C.-G. Zhou, Z. An, and Z.-M. Luo, Chin. Phys. Lett. **18**, 759 (2001).
12. A. Kahoul *et al.*, Radiat. Phys. Chem. **80**, 369 (2011).
13. D. Bote and F. Salvat, Phys. Rev. A **77**, 042701 (2008).
14. D. Bote *et al.*, At. Data Nucl. Data Tables **95**, 871 (2009); D. Bote *et al.*, At. Data Nucl. Data Tables **97**, 186 (2011).
15. E. Casnati, A. Tartari, and C. Baraldi, J. Phys. B **15**, 155 (1982).
16. C. Jakoby, H. Genz, and A. Richter, J. Phys. Colloq. **48**, 487 (1987).
17. C. Hombourger, J. Phys. B, At. Mol. Opt. Phys. **31**, 3693 (1998).
18. C.-H. Tang *et al.*, Chin. Phys. Lett. **18**, 1053 (2001).
19. A. K. F. Haque *et al.*, Phys. Rev. A **73**, 012708 (2006).
20. A. K. F. Haque *et al.*, Eur. Phys. J. D **42**, 203 (2007).
21. B. Gstir *et al.*, J. Phys. B **34**, 3377 (2001).
22. Z. An, Z. M. Luo, and C. Tang, Nucl. Instrum. Methods Phys. Res. B **179**, 334 (2001).
23. A. K. F. Haque *et al.*, Int. J. Quantum Chem. **109**, 1442 (2009).
24. A. K. F. Haque *et al.*, J. Phys. B **43**, 115201 (2010).
25. J. P. Santos, F. Parente, and Y.-K. Kim, J. Phys. B: At. Mol. Opt. Phys. **36**, 4211 (2003).
26. M. Guerra *et al.*, Int. J. Mass Spectrom. **313**, 1 (2012).
27. M. Gryziński, Phys. Rev. **138**, A322 (1965).
28. J. H. Scofield, Phys. Rev. A **18**, 963 (1978).
29. H. Kolbenstvedt, J. Appl. Phys. **46**, 2771 (1975).
30. Md. R. Khan and M. Karimi, X-Ray Spectrom. **9**, 32 (1980); M. Ertuğrul *et al.*, J. Phys. B **34**, 909 (2001); J. P. Marques, F. Parente, and P. Indelicato, J. Phys. B **34**, 3487 (2001).
31. H. K. Chung *et al.*, High Energy Density Phys. **1**, 3 (2005).
32. H. O. Wyckoff, *ICRU Report*, International Commission on Radiation Units and Measurements, Inc., Bethesda, MD (1984).
33. ESTAR, accessed 16 May 2013, <http://physics.nist.gov/PhysRefData/Star/Text/ESTAR.html>.
34. R. M. Sternheimer, M. J. Berger, and S. M. Seltzer, At. Data Nucl. Data Tables **30**, 261 (1984).
35. S. Atzeni, A. Schiavi, and J. R. Davies, Plasma Phys. Control. Fusion **51**, 015016 (2009).
36. EGSnrc Monte Carlo code, accessed 17 May 2013, <http://www.nrc-cnrc.gc.ca/eng/rd/mss/index.html>.
37. XCOM, accessed 16 May 2013, <http://physics.nist.gov/PhysRefData/Xcom/html/xcom1.html>.
38. A. Kahoul *et al.*, Radiat. Phys. Chem. **80**, 369 (2011).
39. PSTAR, accessed 16 May 2013, <http://physics.nist.gov/PhysRefData/Star/Text/PSTAR.html>.
40. J. P. Desclaux, At. Data Nucl. Data Tables **12**, 311 (1973).